Use of $\pi p \to \pi\pi N$ reactions to study $\pi\pi$ scattering in the elastic-interaction region

E. A. Alekseeva, A. A. Kartamyshev, V. K. Makar'in, K. N. Mukhin, O. O. Patarakin, M. M. Sulkovskaya, A. F. Sustavov, L. V. Surkova, and L. A. Chernysheva

I. V. Kurchatov Institute of Atomic Energy
(Submitted 3 February 1981)
Zh. Eksp. Teor. Fiz. **82**, 1007–1025 (April 1982)

$\pi\pi$ scattering is investigated in the region where it can be regarded as elastic. Information is used on four different channels of a reaction of the type $\pi p \to \pi\pi N$. A single procedure is used to obtain for all the essential $\pi\pi$-scattering phase shifts in the investigated region, $\delta_0{}^0$, $\delta_0{}^2$, δ_1^1, $\delta_2{}^0$, and $\delta_2{}^2$, values that are in good agreement with one another. A continuous plot of $\delta_0{}^0$ from threshold to 980 MeV is obtained. It is shown that it is incorrect to apply the effective-radius approximation to S-wave phase shifts at $m_{\pi\pi} \geq 400$ MeV. The hypothesis that close near-threshold zeros are present in the S-wave amplitudes is proved experimentally. The positions of the zeros are found. Analytic, unitary, and crossing-symmetry partial $\pi\pi$ amplitudes are determined, which satisfy the Roy equations and agree well with the phase-shift-analysis results. It is concluded that the lower "down" solution is preferable for the $\delta_0{}^0$ phase shift. The scattering lengths of the S, P, and D waves are obtained.

PACS numbers: 13.75.Lb, 13.75.Gx

1. INTRODUCTION

More than 20 years have elapsed since the appearance of the first papers on the $\pi\pi$ interaction, but developments in this field continue to this day. The $\pi\pi$ interaction is of interest apparently because it is very frequently encountered, it is relatively easy to describe theoretically, and is a nonstandard procedure for obtaining experimental information.

$\pi\pi$ scattering enters in a large number of diagrams and determines a large group of phenomena. The small mass and zero spin of the pion, as well as the complete crossing symmetry of the $\pi\pi$ scattering, make processes of the type $\pi\pi \to \pi\pi$ quite sensitive to theoretical predictions. In particular, an exceedingly important role is played by these processes in dual models: $\pi\pi$-resonance spectroscopy is needed to check on the predictions of these models. Complete crossing symmetry of the $\pi\pi$ scattering makes it the best candidate for the use of models in which the principles of analyticity, unitarity, and crossing symmetry are used. Progress in this field is due to the equations of Roy, which will be dealt with later. The study of $\pi\pi$ interaction at low energies is of particular interest because of the possibility of comparison with the predictions of current algebra and of models with broken chiral symmetry, and of checking the partial conservation of axial current (PCAC) hypothesis. In addition, interest in this field has increased recently in connection with the development of the theory of π-condensate and of the anomalous state of nuclear matter. Exact calculations in such models also require data on $\pi\pi$ scattering.

In the absence of colliding pion beams and meson targets, information on the $\pi\pi$ interaction can be obtained only by indirect methods. In principle, a possible source of information can be any process that includes the $\pi\pi$ interaction. The most important sources of formation are at present the production of several pions upon irradiation of a very simple target (proton, deuteron) by a pion beam ($\pi N \to \pi\pi N$, $\pi N \to \pi\pi\Delta$).

In these reactions, at a small four-momentum transfer t, the one-pion exchange (OPE) diagram predominates. In the presence of sufficient statistics, it becomes possible to separate the contribution of the OPE diagram and, by studying the scattering of a real pion by a virtual one, proceed to a description of the process in the pion pole, i.e., to scattering of real mesons. Study of reactions of the type $\pi N \to \pi\pi N$ makes it possible in principle to obtain complete information on all the possible states of a $\pi\pi$ system in the entire region of dipion masses $m_{\pi\pi}$.

The present paper is devoted to the study of $\pi\pi$ scattering in a region in which this interaction can be regarded as elastic ($\eta_l^I = 1$). Strictly speaking, the region of elastic interaction is bounded by the 4π threshold, $m_{\pi\pi} = 560$ MeV. In practice, however, the $\pi\pi$ interaction can be regarded as elastic at much larger $m_{\pi\pi}$. Thus, $\pi^-\pi^+ \to \pi^-\pi^+$ scattering remains practically elastic up to the $K\bar{K}$ threshold, $m_{\pi\pi} = 960$ MeV, while $\pi^\pm\pi^0 \to \pi^\pm\pi^0$ and $\pi^\pm\pi^\pm \to \pi^\pm\pi^\pm$ remain so even up to $m_{\pi\pi} \approx 1200$ MeV. Many recent papers, e.g., Refs. 1–4, based on abundant statistical material, are devoted to the study of $\pi\pi$ interaction. The main emphasis in these papers, however, is on the large-mass region, $m_{\pi\pi} > 1$ GeV. Yet a number of unsolved problems still remain in the elastic interaction region: there is no reliable agreement between the values of the S_0-wave phase shift obtained near threshold also at larger $m_{\pi\pi}$, the uncertainty in the behavior of the phase shift $\delta_0{}^0$ in the region of the ρ resonance (the "up-down" ambiguity) was not resolved, contradictory data were obtained on the $\pi\pi$ scattering lengths, and others.

To obtain information on the $\pi\pi$ interactions we used reactions of the type $\pi p \to \pi\pi N$. Since the study of any particular charge channel does not yield all the possible amplitudes, we used data on four different channels. This has made it possible to obtain by a single procedure all the $\pi\pi$ scattering phase shifts that are of importance in the investigated $m_{\pi\pi}$ region. We used for

TABLE I.

Reaction	Momentum GeV/c	No. of events	Reaction	Momentum GeV/c	No. of events
$\pi^- p \to \pi^- p$	4.5	5936	$\pi^+ p \to \pi^+ p$	3.05	5615
$\pi^- p \to \pi^- \pi^+ n$	4.5	12500	$\pi^+ p \to \pi^+ \pi^0 p$	3.05	2600
$\pi^- p \to \pi^- \pi^0 p$	4.5	4900	$\pi^+ p \to \pi^+ \pi^+ n$	3.05	3300

this purpose $\pi p \to \pi\pi N$ events obtained by bombarding a liquid-hydrogen bubble chamber with pions[5-9] (see Table I). Problems involving the identification of the events and their measurements are described in Ref. 10.

The available materials yielded the $\pi\pi$ scattering phase shifts in the elastic-interaction region for $m_{\pi\pi}$ >370 MeV, and enabled us also to extrapolate the results to the threshold and determine the scattering lengths. In addition, to study the region of small $m_{\pi\pi}$ we used 496 events of the reaction $\pi^- p \to \pi^- \pi^+ n$, obtained in the JINR by an emulsion method at an incident pion energy T_π = 200–260 MeV.[11] This yielded for one and the same reaction and by a unified reduction procedure a continuous curve for the phase shift δ_0^0 from threshold to m_π = 960 MeV.

2. DETERMINATION OF THE CHARACTERISTICS OF THE REACTIONS $\pi^\pm p \to \pi^\pm p$, $\pi^\pm p \to \pi^\pm \pi^+ n$, $\pi^\pm p \to \pi^\pm \pi^0 p$

2.1. Elastic $\pi^\pm p$ scattering

The study of elastic scattering makes it possible not only to investigate this process but also to obtain a normalization cross section for the other $\pi\pi$ interaction channels.

In the measurement and reduction of the elastic-scattering events, short proton tracks on the photograph are sometimes lost. This occurs when the proton momentum is small or is directed towards the cameras. A correction must be introduced for these missed counts. This correction depends on the azimuthal angle φ and on the pion scattering angle θ. The procedure for obtaining the correction coefficients and the results of an investigation of elastic $\pi^\pm p$ scattering are described in Ref. 10. Using the optical theorem, we can obtain the total number of reaction events, the normalized cross section per event, and the cross sections of the reactions:

$$\sigma(\pi^- p \to \pi^- p) = 6.21 \pm 0.19 \text{ mb at } p_{\pi^-} = 4.5 \text{ GeV}/c;$$
$$\sigma(\pi^+ p \to \pi^+ p) = 7.02 \pm 0.23 \text{ mb at } p_{\pi^+} = 3.05 \text{GeV}/c.$$

2.2 The reaction $\pi^- p \to \pi^- \pi^+ n$

The azimuthal distributions show that no missed counts occur in the events of the reaction $\pi^- p \to \pi^- \pi^+ n$. The reason is that in this case the measured pion tracks are much longer than the proton tracks. The cross section of the reaction was found to be

$$\sigma(\pi^- p \to \pi^- \pi^+ n) = 3.04 \pm 0.20 \text{ mb at } p_{\pi^-} = 4.5 \text{ GeV}/c.$$

The reaction $\pi^- p \to \pi^- \pi^+ n$ can proceed via resonant states of two pions or of a pion and a neutron, i.e., through the production of ρ^0-,f^0-,g^0-, $\Delta^\pm$ resonances.
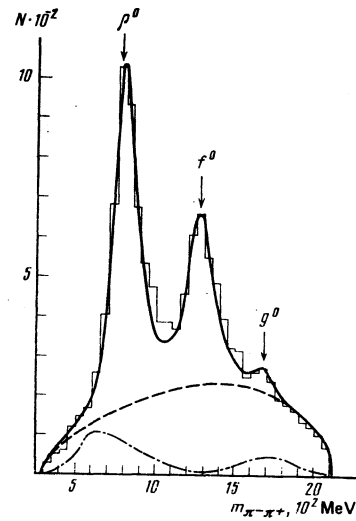

FIG. 1. Distribution of the events of the reaction $\pi^- p \to \pi^- \pi^+ n$ in $m_{\pi\pi}$. The dash-dot curve shows the reflection of the $\Delta(1232)$ resonance, magnified 5 times, the dashed lines show the phase volume, and the solid curve is the sum of the Breit-Wigner curves for the ρ^0, f^0, and g^0 resonances, the phase volume, and the $\Delta(1232)$ reflection.

Although the cross section for the production of the $\Delta^\pm$ isobar is small at our energy, this resonance influences the distribution of the events in the dipion effective mass $m_{\pi\pi}$. The reflection of the isobars from the pion resonances can be taken into account by using the equation[12]

$$F_{ref}(m_{\pi\pi}^2) = \int_{(m_{\pi N}^2)_{min}}^{(m_{\pi N}^2)_{max}} F_{res} \psi(\cos\theta) \frac{dm_{\pi N}^2}{B(m_{\pi N}^2)}, \tag{1}$$

where F_{res} is the Breit-Wigner form of the Δ isobar, $\psi(\cos\theta) = N^{-1}dN/d\cos\theta$ is the angular distribution of the Δ decay products, and

$$B(m_{\pi N}^2) = \frac{1}{2m_{\pi N}^2}\{[(E_c+m_\pi)^2-m_{\pi N}^2][(E_c-m_\pi)^2-m_{\pi N}^2]$$
$$\times[m_{\pi N}^2-(m_\pi+m_n)^2][m_{\pi N}^2-(m_n-m_\pi)^2]\}^{1/2},$$

where E_c is the total energy in the c.m.s.

From the angular-momentum and parity conservation laws it follows that the Δ resonance decays into a neutron and a pion in the P state, for which $\psi(\cos\theta) \sim \cos^2\theta$.

The distribution in $m_{\pi^-\pi^+}$ was approximated by a sum of five curves: of the invariant phase volume, of the Breit-Wigner curves for the ρ^0, f^0, and g^0 resonances, and of the Δ-isobar reflection (see Fig. 1). This has made it possible to determine the parameters of the resonances and their cross sections. The obtained values are given in Table II.

TABLE II.

Resonance	$m_{\pi\pi}$, MeV	Γ, MeV	σ, mb	p, GeV/c
ρ^-	790±15	180±15	0.50±0.04	4.5
ρ^0	790±10	170±10	0.85±0.05	4.5
ρ^+	780±15	140±15	1.07±0.11	3.05
f^0	1270±20	200±30	0.52±0.04	4.5
g^-	1680±20	190±25	0.03±0.03	4.5
g^0	1680±20	190±25	0.05±0.05	4.5
$\Delta^\pm$	1232 (fixed)	120 (fixed)	0.06±0.02	4.5

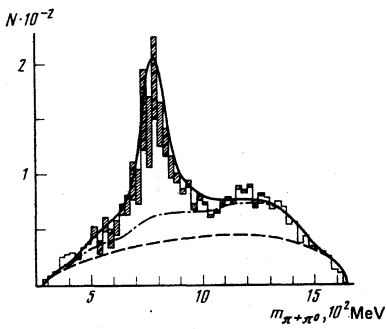FIG. 2. Distribution in the effective mass $m_{\pi\pi}$ for the reaction $\pi^+p \to \pi^+\pi^0 p$. Dashed line—phase volume, dash-dot—sum of reflection of the Δ resonances and of the phase volume, solid curve—sum of the Breit-Wigner ρ^+ resonance, phase volume, and reflection. The shaded part of the histogram shows the corrections for the missed counts.

2.3. The reaction $\pi^\pm p \to \pi^\pm \pi^0 p$

Missed counts take place for the reactions $\pi^\pm p \to \pi^\pm\pi^0 p$, as indicated by the azimuthal distributions. After taking these missed counts into account, the following reaction cross sections were obtained:

$$\sigma(\pi^- p \to \pi^-\pi^0 p)$$
$$=2.01\pm0.16 \text{ mb at}$$
$$p_{\pi^-}=4.5 \text{ GeV}/c;$$
$$\sigma(\pi^+ p \to \pi^+\pi^0 p)$$
$$=3.26\pm0.24 \text{ mb at}$$
$$p_{\pi^+}=3.05 \text{ GeV}/c.$$

The parameters of the $\rho^\pm$ and the g^- resonances, obtained with account taken of the Δ-isobar reflection, are given in Table II. The obtained description of the experimental distribution is shown in Fig. 2. For $\pi^- p \to \pi^-\pi^0 p$ the contribution from the $\Delta^\pm$ isobar is small, and for the reaction $\pi^+ p \to \pi^+\pi^0 p$ at $p_{\pi^+}=3.05$ GeV/c the contribution of the Δ isobars amounts to $\sigma_\Delta = 0.73 \pm 0.15$ mb. Using the isotopic relation $\sigma_{\Delta^+} = \frac{4}{9}\sigma_{\Delta^{++}}$, we can obtain $\sigma_{\Delta^+} = 0.22\pm0.05$ mb; $\sigma_{\Delta^{++}} = 0.51\pm0.11$ mb at $p_{\pi^+}= 3.05$ GeV/c.

2.4 The reaction $\pi^+ p \to \pi^+\pi^+ n$

The cross section of this reaction is $\sigma(\pi^+p \to \pi^+\pi^+ n) = 2.18\pm0.16$ mb at $p_{\pi^+}= 3.05$ GeV/c. The mass distributions of $m_{\pi\pi}$ and $m_{\pi N}$ are well described by the phase shift curves. The contribution of the Δ^+ resonance can be estimated from the relation $\sigma_{\Delta^+}(\pi^+\pi^+ n) = \frac{2}{9}\sigma_{\Delta^{++}}(\pi^+\pi^0 p)$, whence $\sigma_{\pi^+}= 0.12$ mb, which amounts to ~5% of the total cross section.

3. PREPARATION OF THE DATA FOR THE PHASE-SHIFT ANALYSIS

In the reaction $\pi^- p \to \pi^-\pi^+ n$, we selected for further processing events with $|t| \le 0.3$ (GeV/c)^2. This restriction is imposed by the fact that the main background in this reaction is due to A_2 exchange. As shown, e.g., by Kimel and Reya,[13] allowance for the background becomes important at $|t| \gtrsim 0.25$ (GeV/c)^2. The calculations were performed for $p_\pi= 17$ GeV/c, and for a smaller momentum the contribution of the A_2 exchange

should decrease compared with the π exchange. The same restriction $|t| \le 0.3$ (GeV/c)^2 was imposed also on the events of the reaction $\pi^- p \to \pi^-\pi^0 p$, but for this reaction we introduced one more restriction: $|t| \ge 0.08$ (GeV/c)^2. This was due to the presence of missed events with short proton tracks, i.e., with small $|t|$, which are difficult to take into account. This additional restriction, however, has also a favorable aspect: the ω exchange is largest precisely for $|t| \lesssim 0.1$ (GeV/c)^2 (Ref. 14). It is difficult to take the ω exchange into account in explicit form, so that it is useful to decrease its contribution.

The statistics for reactions with positive incident pions was smaller, it was therefore desirable to extend the employed region to $|t| \le 0.5$ (GeV/c)^2. To get rid in this case of the large percentage of admixtures of other diagrams, the selection was based on the van Hove angle ω (Ref. 15). This angle is defined as

$$\omega = \text{arctg}\left(-\frac{3^{\frac{1}{2}}q_N}{q_{\pi^+}-q_{\pi^0}}\right), \quad (2)$$

where q_i is the longitudinal momentum of the particle i in the c.m.s.

As shown in Ref. 16, one-pion exchange corresponds to a definite sector which amounts in the coordinate system chosen by us to $240° \le \omega \le 300°$. The selection of events in accord with the angle ω yields good results for a sufficiently large initial momentum, and at our momentum $p_\pi = 3$ GeV/c one should expect a smearing of the boundaries and intermixing of events due to different mechanisms within a single sector. One can assume nevertheless that the region $225° \le \omega \le 315°$ is enriched with events of the OPE exchange type and extrapolation of these events yields correct results. It should be noted that events with $|t| < 0.3$ (GeV/c)^2 practically all land in the chosen sector (at least at $m_{\pi\pi} < 1100$ MeV).

An important question is the allowance for the isobar formation in the final state. Whereas for the reaction with $p_{\pi^-}= 4.5$ GeV/c no noticeable contribution of the isobars was observed, for $p_{\pi^+}= 3.05$ GeV/c the cross section for the production of $\Delta^+(1232)$ and especially $\Delta^{++}(1232)$ is quite large. Therefore events with $1185 < m_{\pi N} < 1285$ MeV were not used in the subsequent analysis.

Table III lists the number of events remaining after all the restrictions are imposed.

Practically all extrapolations of the data to the pion pole are based on the old Chew-Low formula,[17] which connects the cross section $\sigma_{\pi\pi}$ with the differential cross section of the reaction $\pi N \to \pi\pi N$:

$$\sigma_{\pi\pi}(m_{\pi\pi}) = \lim_{t\to\mu^2}\left[\frac{\partial^2\sigma_{\pi\pi N}}{\partial t \partial m_{\pi\pi}}\frac{\pi}{\alpha f^2}\frac{p^2(t-\mu^2)^2}{tm_{\pi\pi}k}\right]. \quad (3)$$

TABLE III.

Reaction	No. of events	$\Delta m_{\pi\pi}$
$\pi^- p \to \pi^-\pi^+ n$	3011	$320 \le m_{\pi\pi} \le 980$ MeV
$\pi^- p \to \pi^-\pi^0 p$	1315	$387 \le m_{\pi\pi} \le 1215$ MeV
$\pi^+ p \to \pi^+\pi^0 p$	1151	$387 \le m_{\pi\pi} \le 1215$ MeV
$\pi^+ p \to \pi^+\pi^+ n$	1555	$387 \le m_{\pi\pi} \le 1215$ MeV

593   Sov. Phys. JETP 55(4), April 1982

Alekseeva et al.   593

Here α is a numerical coefficient equal to 1 for $\pi p \rightarrow \pi^\pm\pi^0 p$ and to 2 for $\pi p \rightarrow \pi\pi n$, $f^2 = 0.08$ is the πN interaction constant, p_π is the momentum of the incident pion, $k = (m_{\pi\pi}^2/4 - \mu^2)^{1/2}$ is the momentum of the secondary pion in the rest system of the dipion, and $\mu \equiv m_\pi$.

To obtain the value of the pion-pion cross section, one usually constructs the auxiliary function

$$F(t) = \frac{\partial^2\sigma}{\partial t\,\partial m_{\pi\pi}}\frac{2\pi p_\pi^2(t-\mu^2)^2}{\alpha f^2 m_{\pi\pi}k}. \qquad (4)$$

This function is extrapolated to the pole where

$$\sigma_{\pi\pi}(m_{\pi\pi}) = \lim F(t, m_{\pi\pi})/t \quad (t\rightarrow\mu^2).$$

In the present paper we used the pseudoperipheral-approximation method proposed by Baton et al.[18] It is assumed additionally in it that $F(0) = 0$, and an auxiliary function $F'(t) = F(t)/t$ is constructed, and it is this which is extrapolated to the pole. Figure 3 shows the values of $\sigma_{\pi\pi}$ obtained for all the charge states.

In the phase-shift analysis we need the angular characteristics of the secondary pions, which must be known for the scattering of real pions. In the present paper the angular distributions are described by averaged spherical harmonics $\langle Y_L^0\rangle(m_{\pi\pi})$ extrapolated to the pion pole:

$$\langle Y_L^0\rangle(m_{\pi\pi}, t) = \frac{1}{N}\sum_{i=1}^{N} Y_L^0(\theta_i, m_{\pi\pi}, t), \qquad (5)$$

where N is the number of events in the considered interval $\Delta m_{\pi\pi}$, Δt. We recall the connection between $\langle Y_L^0\rangle$ and the phase shifts for the case $l \leq 2$:
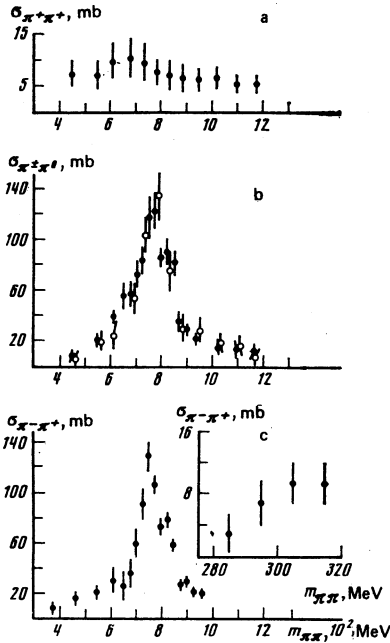
FIG. 3. Values of the pion-pion cross sections for the different charge channels: a) $\pi^+\pi^+\rightarrow\pi^+\pi^+$; b) $\pi^-\pi^0\rightarrow\pi^-\pi^0$ (points) and $\pi^+\pi^0\rightarrow\pi^+\pi^0$ (circles); c) $\pi^-\pi^+\rightarrow\pi^-\pi^+$; the insert shows the values of $\sigma_{\pi\pi}$ near threshold, obtained from an analysis of emulsion data of the reaction $\pi^-p\rightarrow\pi^-\pi^+n$ at $200 \leq T_\pi \leq 260$ MeV.
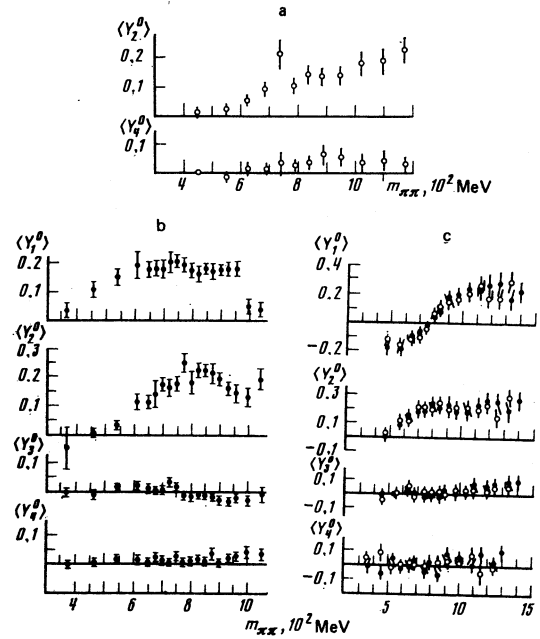
FIG. 4. Extrapolated values of the averaged spherical harmonics $\langle Y_L^0\rangle$ $(m_{\pi\pi})$, $L = 1, \ldots, 4$ for a) $\pi^+\pi^+\rightarrow\pi^+\pi^+$ scattering; b) $\pi^-\pi^+\rightarrow\pi^-\pi^+$ scattering; c) $\pi^-\pi^0\rightarrow\pi^-\pi^0$ scattering (points) and $\pi^+\pi^0\rightarrow\pi^+\pi^0$ scattering (circles).

$$\sigma_{\pi\pi} = 4\pi\lambda^2\{|S|^2+3|P|^2+5|D|^2\},$$

$$\langle Y_1^0\rangle = \frac{4\pi\lambda^2}{\sigma_{\pi\pi}}\left\{\sqrt{\frac{3}{\pi}}\,\text{Re}(S^*P)+2\sqrt{\frac{3}{\pi}}\,\text{Re}(P^*D)\right\},$$

$$\langle Y_2^0\rangle = \frac{4\pi\lambda^2}{\sigma_{\pi\pi}}\left\{\frac{3}{\sqrt{5\pi}}|P|^2+\sqrt{\frac{5}{\pi}}\,\text{Re}(S^*D)+\frac{5}{7}\sqrt{\frac{5}{\pi}}|D|^2\right\}, \qquad (6)$$

$$\langle Y_3^0\rangle = \frac{4\pi\lambda^2}{\sigma_{\pi\pi}}\frac{9}{\sqrt{7\pi}}\,\text{Re}(P^*D),$$

$$\langle Y_4^0\rangle = \frac{4\pi\lambda^2}{\sigma_{\pi\pi}}\frac{15}{7\sqrt{\pi}}|D|^2,$$

where $S = \frac{2}{3}A_0^0 + \frac{1}{3}A_0^2$, $P = A_1^1$, $D = \frac{2}{3}A_2^0 + \frac{1}{3}A_2^2$. The investigated region of the dipion masses was such that the elastic interaction can be correctly represented by $A_l^I = \sin\delta_l^I \exp\{i\delta_l^I\}$.

Figure 4 shows the values of $\langle Y_L^0\rangle(m_{\pi\pi})$, $L = 1, \ldots, 4$ for different charge states of the dipion. The form of $\langle Y_1^0\rangle$ for the $\pi^\pm\pi^0$ state is characteristic. Being negative at small $m_{\pi\pi}$, $\langle Y_1^0\rangle$ reverses sign at $m_{\pi\pi}\approx 780$ MeV. It is clear that this sign reversal is determined by the term with $\cos(\delta_1^1 - \delta_0^2)$, which reverses sign when $(\delta_1^1 - \delta_0^2)$ goes through $90°$. Knowing that the δ_1^1 phase shift is positive and is determined by the ρ resonance with mass $m_{\pi\pi}\sim 750$ MeV, we find directly that the δ_0^2 phase shift is negative and small.

The quantity $\langle Y_2^0\rangle$ is everywhere positive, including in the $\pi^+\pi^-$ interaction. Since there is no P_1 wave in this interaction, it can be concluded that the signs of δ_0^2 and δ_2^2 are equal. From the smallness of $\langle Y_3^0\rangle$ and $\langle Y_4^0\rangle$ it is seen that the D-wave amplitudes are small in the elastic region.

The behavior of $\langle Y_1^0\rangle$ for $\pi^+\pi^+$ scattering is very interesting. In the region of the KK threshold one can

see an abrupt drop, almost to zero. Since there is no such drop in $\langle Y_1^0 \rangle$ for the $\pi^\pm \pi^0$ scattering, just as there are no singularities of $\langle Y_2^0 \rangle$ in this region (P_1 wave), it is natural to assume that the drop is connected with the S_0 wave. Indeed, it has now become generally customary to explain this anomaly in the behavior of $\langle Y_1^0 \rangle$ with the aid of the S^* (1000) meson. This behavior of $\langle Y_1^0 \rangle$ provides a weighty argument in favor of choosing the lower "down" solution for the δ_0^2 phase shift. It is seen that even from the outward form of the harmonics one can discern much that is of interest, but of course the quantitative conclusions can be drawn only from a physical analysis.

4. PHASE-SHIFT ANALYSIS OF $\pi\pi$ SCATTERING

We used in this study both an energy-independent and an energy-dependent phase-shift analysis method. In the energy-independent analysis, the data for different $m_{\pi\pi}$ are analyzed separately, and the solutions for the phase shifts and the elasticity coefficients are obtained separately for each mass interval. Waves with angular momentum exceeding a certain l_{max} are assumed to be negligibly small, and the parameters of the remaining waves (with $l \leq l_{max}$) are assumed free within the unitarity framework. In the energy-dependent analysis, all the data for the different energies are described jointly, using for this purpose an energy-dependent parametrization of the partial amplitudes. This method yields a smooth solution, and the statistical deviations at individual points manifest themselves less. Of course, it is necessary to choose the parametrization correctly, otherwise large systematic errors are possible.

We consider separately the results obtained by both analysis method. When using the energy-independent analysis, the system of equations for $\sigma_{\pi\pi}$ and for the $\langle Y_L^0 \rangle$ extrapolated to the pion pole was solved by an iteration method with the phase-shifts δ_L^I as the free parameters.

A study of the $\pi^+\pi^+ \to \pi^+\pi^+$ scattering via the reaction $\pi^+ p \to \pi^+\pi^+ n$ has made it possible to determine the phase shifts of the waves with $I = 2$. We used the results obtained for 1600 events with $|t| \leq 0.5$ (GeV/c)^2 and $225° \leq \omega \leq 315°$, for in the case of simple cutoff in $|t|$ there remains the danger of failing to eliminate to a sufficient degree the contribution from the isobar production and from the diffractive-dissociation processes. Selection based on the van Hove angle seems more promising, since it adds the one-pion exchange events to the events used for the extrapolation.

The study of the $\pi^+\pi^0$ and $\pi^-\pi^0$ states is of interest not only because it is possible to obtain δ_1^1 and δ_2^2, but also for the possibility of estimating the influence of small contributions from the higher waves with the D_2 wave as the example. It has turned out that despite the smallness of δ_2^2 in the investigated region, it cannot be neglected even at $m_{\pi\pi} < 900$ MeV, because of the considerable S_2-D_2 and P_1-D_2 interference.

The greatest interest attaches to the study of $\pi^-\pi^+ \to \pi^-\pi^+$ scattering in which all possible waves are pres-
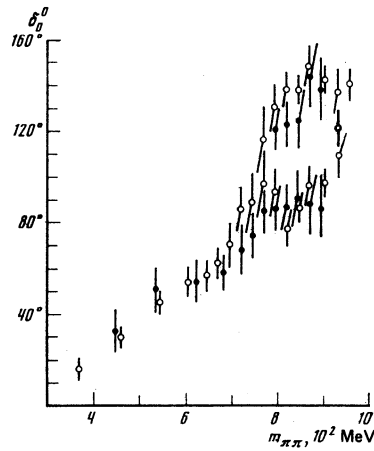

FIG. 5. Two versions of the calculations for the phase shift δ_0^0, obtained by the energy-independent method from the reaction $\pi^- p \to \pi^-\pi^+ n$ at $p_\pi = 4.5$ GeV/c.

ent. It is impossible to obtain simultaneously phase shifts with identical spin by studying one channel, therefore the phase shifts δ_2^2 and δ_0^2 were determined from $\pi^+\pi^+$ scattering data. It is known that the solution for δ_0^2 has an ambiguity of the form $\delta_0^{0\prime} = \delta_1^1 + (\pi/2 - \delta_0^0)$. At $m_{\pi\pi} < 750$ MeV, it is easy to choose the solution by comparison with $\sigma_{\pi\pi}$, but in the region $750 < m_{\pi\pi} < 950$ MeV, where σ_P is substantially larger than σ_S, the choice of the solution is a rather complicated matter. We discuss the problem in greater detail below. Figure 5 shows the obtained values of the δ_0^0 phase shift.

In the energy-dependent analysis we minimized a functional of the form

$$W = \sum_{I=1}^{N} \left(\frac{\sigma_I^{theor} - \sigma_I^{exp}}{\Delta\sigma_I^{exp}} \right)^2 + \sum_{L=1}^{4} \sum_{I=1}^{N} \left(\frac{\langle Y_L^0 \rangle_I^{theor} - \langle Y_L^0 \rangle_I^{exp}}{\Delta\langle Y_L^0 \rangle_I^{exp}} \right)^2 . \quad (7)$$

The simplest parametrization was used for waves with $I = 2$. For the δ_2^2 phase shift we used power-law series in $m_{\pi\pi}$ and q, e.g.,

$$\delta_2^2(q) = \sum_{j=0}^{k} \beta_j q^{2j+1},$$

where $k = 2$ and 3. For the S-wave phase shifts we used, besides the power-law series, the effective-radius formula as well as the Serebryakov formula,[19] which takes into account the existence of a subthreshold zero in the S-wave amplitudes:

$$\delta_0^I = \text{arcctg} \left(\frac{m_{\pi\pi}}{2q} \frac{1 + B_0 q^2}{a_0^I + D_0 q^2} \right), \quad (8)$$

where a_0^I is the scattering length, and B_0 and D_0 are free parameters. The P_1 wave, whose behavior determines the ρ resonance, was parametrized by different versions of the Breit-Wigner formula, e.g.,

$$\delta_1^1 = \text{arctg} \left[\frac{m_\rho \Gamma_\rho}{m_\rho^2 - m_{\pi\pi}^2} \left(\frac{q}{q_\rho} \right)^3 \right] . \quad (9)$$

The energy-dependent approach yielded a good description of the experimental points for all the reactions. Besides the energy-dependent analysis of individual charge channels, we carried out a general energy-de-
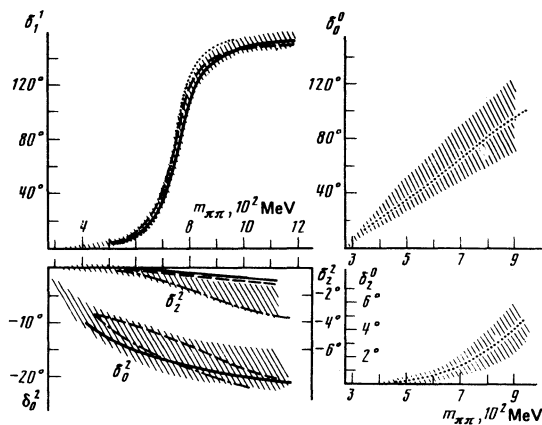
FIG. 6. Results of energy-independent analysis. Shaded region—region of possible values from the complete energy-dependent analysis, lines—results of analysis for separate charge channels: the solid, dash-dot, dashed, and dotted curves correspond to $\pi^+\pi^0$, $\pi^+\pi^+$, $\pi^-\pi^0$, and $\pi^-\pi^+$, respectively.

pendent analysis, in which all the experimental data were described simultaneously. This made it possible to obtain all the $\pi\pi$ scattering phase shifts in the investigated region directly, without fixing any parameters. The shaded region in Fig. 6 shows the region of the general analysis, while the lines show the calculation results for individual channels (the errors are not shown).

5. BEHAVIOR OF $\pi\pi$ SCATTERING AMPLITUDES NEAR THRESHOLD. SCATTERING LENGTHS

Knowing the $\pi\pi$ scattering phase shifts, we can attempt to determine the $\pi\pi$ scattering lengths. We recall that by definition the scattering length is

$$a_l^I = \lim_{q \to 0} \frac{\delta_l^I(q)}{q^{2l+1}}.$$

Naturally, the experimental value of the scattering length depends on the formula used to extrapolate the phases to the threshold. One uses quite frequently for this purpose the effective-radius approximation, which is valid if q is not too large. In the case of the S wave, however, there are long-standing objections to the use of this formula, in view of the possible existence of a threshold zero in the real part of the S-wave amplitude not far from the physical region. In this case the expansion

$$q^{2l+1} \operatorname{ctg} \delta_l^I = F_l^I(q^2) = \frac{1}{a_l^I} + \frac{1}{2} q^2 r_l^I + O(q^4) \tag{10}$$

has a very small convergence radius, while a direct extrapolation of the quantity $F_l^I(q^2)$ from the physical region does not take into account its abrupt growth near zero, and leads to an overestimate of the scattering length. This was pointed out, e.g., in Refs. 20–22. To finally resolve the question of existence of the subthreshold zero, it is desirable to have S-wave phase shifts obtained by the same method both near threshold and in the region of large dipion masses.

Usually the phase shifts of the $\pi\pi$ scattering near the threshold are obtained from an analysis of K_{e4} decays
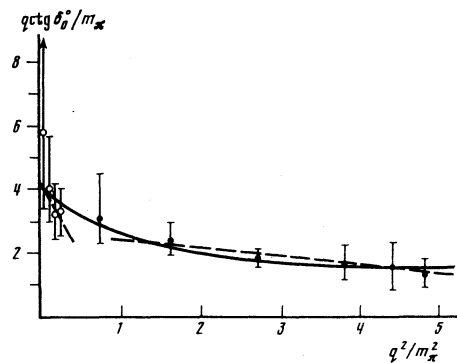

FIG. 7. Behavior of the function $q \cot \delta_0^0(q^2)$. Dashed line—effective-radius approximation for $280 \le m_{\pi\pi} \le 320$ MeV and $450 \le m_{\pi\pi} \le 725$ MeV. Solid line—calculation by a formula that takes the subthreshold zero into account.

by a rather complicated method that requires a large amount of statistical material. It was therefore important to attempt directly near threshold the phase-shift-analysis procedure used to reduce events in the region of large $m_{\pi\pi}$. To do this, 495 events of the reaction $\pi^- p \to \pi^- \pi^+ n$, which were obtained by the emulsion method in the incident-pion kinetic energy $200 \le T_\pi \le 260$ MeV (Ref. 11) were analyzed. This made it possible to obtain the $\pi^-\pi^+$ scattering phase shifts δ_0^0 and δ_1^1 from threshold to $m_{\pi\pi} = 320$ MeV.

Thus, we have obtained in the present paper, using the same reaction $\pi^- p \to \pi^- \pi^+ n$ and the same data-reduction method, the values of δ_0^0 from threshold to $m_{\pi\pi} \approx 1$ GeV. Figure 7 shows the values of the function $q \cot \delta_0^0$. The dashed lines show the results of the effective-radius approximation for the near-threshold region $m_{\pi\pi} < 320$ MeV and the region $450 \le m_{\pi\pi} \le 725$ MeV. One can clearly see a break that confirms the nonlinear behavior of $q \cot \delta_0^0$ in the considered region. The solid line is an approximation of the Serebryakov formula, which takes into account the subthreshold zero. It is seen that the result demonstrates that the linear approximation cannot be used for $m_{\pi\pi} \ge 350$ MeV, and by the same token confirms experimentally the hypothesis that a subthreshold zero exists in the S_0 wave amplitude.

The behavior of the partial amplitudes near the threshold can be analyzed with the aid of models that use the principles of analyticity, unitarity, and crossing symmetry. Very useful for $\pi\pi$ scattering are the exact equations, obtained by Roy,[23,24] using dispersion relations with two subtractions at fixed t and the crossing symmetry properties of the scattering amplitudes. These equations determine the partial wave amplitudes in the region $-4 \le s \le 60$, ($s \equiv m_{\pi\pi}^2/\mu^2$) in terms of the values in the physical region $4 \le s < \infty$. The Roy equations and the unitary relation constitute a system of nonlinear singular equations. This system is convenient to work with and makes it possible in principle to determine the scattering lengths and the positions of the subthreshold zeros, as well as to resolve the "up-down" ambiguity. In the case of charged pions, the Roy equations can be written in the form

$$\operatorname{Re} f_l{}^{I'}(s) = \lambda_l{}^{I'}(s) + \sum_{I'=0}^{2} \sum_{l'=0}^{1} \int_4^N K_{ll'}^{I'I'}(s,s') \operatorname{Im} f_{l'}{}^{I'}(s') ds'$$

$$+ \sum_{I'=0}^{2} \sum_{l'=0}^{1} \int_N^\infty K_{ll'}^{I'I'}(s,s') \operatorname{Im} f_{l'}{}^{I'}(s') ds' + \varphi_l{}^{I}(s), \tag{11}$$

where $\lambda_l{}^{I}(s)$ are the subtraction terms, which take for the S and P waves the following explicit form:

$$\lambda_0{}^0(s) = a_0{}^0 + {}^{1}/_{12}(2a_0{}^0 - 5a_0{}^2)(s-4), \quad \lambda_0{}^2(s) = a_0{}^2 - {}^{1}/_{24}(2a_0{}^0 - 5a_0{}^2)(s-4),$$
$$\lambda_1{}^1(s) = {}^{1}/_{72}(2a_0{}^0 - 5a_0{}^2)(s-4),$$

$\varphi_l{}^{I}(s)$ is the sum of contributions from the higher partial waves with $l \geq 2$. $K_{ll'}^{I'I}(s)$ are the kernels of the integral equations. The number N is chosen such that the Regge representations can be used at $N < s < \infty$.

When comparing the quantities that enter in the Roy equations, it was found that the principal role is played by integrals over the region $4 < s' < N$ for $l < 2$ (Refs. 25, 26), while for contributions from the terms with $l \geq 2$ and $N < s' < \infty$ one can get along with an estimate that is not very accurate. We used the estimate of these contributions from Ref. 26. The solutions of the Roy equations differ most strongly from one another in the region of small s, so that to work with them it is desirable to have experimental information in this region. In the present study we had this information for the most important S_0-wave phase shift, and could therefore obtain reliable results.

To find S- and P-wave amplitudes that satisfy the Roy equations and correspond to the experimental data, we calculated $\operatorname{Im} f_l{}^{I}(s)$ and substituted them in the Roy equations represented in the form

$$\operatorname{Re} f_0{}^0(s) = \lambda_0{}^0(s) + \frac{s-4}{\pi} \int_4^{47} \frac{\operatorname{Im} f_0{}^0(x)}{(x-s)(x-4)} dx + \frac{2}{\pi} \int_4^{47} \frac{dx}{x} \left[\frac{x}{s-4} \ln \frac{x+s-4}{x} - 1 \right]$$

$$\times \left[\frac{1}{3} \operatorname{Im} f_0{}^0(x) + \frac{5}{3} \operatorname{Im} f_0{}^2(x) + 3\left(1 + \frac{2s}{x-4}\right) \operatorname{Im} f_1{}^1(x) \right]$$

$$- \frac{s-4}{3\pi} \int_4^{47} \frac{dx}{x(x-4)} [2 \operatorname{Im} f_0{}^0(x) - 9 \operatorname{Im} f_1{}^1(x) - 5 \operatorname{Im} f_0{}^2(x)]$$

$$+ (13 \pm 5) \cdot 10^{-5}(s^2 - 16), \tag{12}$$

$$\operatorname{Re} f_0{}^2(s) = \lambda_0{}^2(s) + \frac{s-4}{\pi} \int_4^{47} \frac{\operatorname{Im} f_0{}^2(x)}{(x-s)(x-4)} dx + \frac{2}{\pi} \int_4^{47} \frac{dx}{x} \left[\frac{x}{s-4} \ln \frac{x+s-4}{x} - 1 \right]$$

$$\times \left[\frac{1}{3} \operatorname{Im} f_0{}^0(x) + \frac{1}{6} \operatorname{Im} f_0{}^2(x) - \frac{3}{2}\left(1 + \frac{2s}{x-4}\right) \operatorname{Im} f_1{}^1(x) \right]$$

$$- \frac{s-4}{6\pi} \int_4^{47} \frac{dx}{x(x-4)} [2 \operatorname{Im} f_0{}^0(x) - 9 \operatorname{Im} f_1{}^1(x) - 5 \operatorname{Im} f_0{}^2(x)]$$

$$+ (13 \pm 6) \cdot 10^{-5} s(s-4),$$

$$\operatorname{Re} f_1{}^1(s) = \lambda_1{}^1(s) + \frac{s-4}{\pi} \int_4^{47} \frac{dx \operatorname{Im} f_1{}^1(x)}{(x-s)(x-4)}$$

$$+ \frac{4}{\pi(s-4)} \int_4^{47} dx \left[\frac{s-4+2x}{2(s-4)} \ln \frac{x+s-4}{x} - 1 \right]$$

$$\times \left[\frac{1}{3} \operatorname{Im} f_0{}^0(x) + \frac{3}{2}\left(1 + \frac{2s}{x-4}\right) \operatorname{Im} f_1{}^1(x) - \frac{5}{6} \operatorname{Im} f_0{}^2(x) \right]$$

$$- \frac{s-4}{18\pi} \int_4^{47} \frac{dx}{x(x-4)} [2 \operatorname{Im} f_0{}^0(x) + 27 \operatorname{Im} f_1{}^1(x) - 5 \operatorname{Im} f_0{}^0(x)]$$

$$+ (3.0 \pm 1.5) \cdot 10^{-5} s(s-4).$$

Since we are interested primarily in the near-threshold region of small s, the accuracy of the estimates is sufficient. For a direct use of these equations it was

necessary to know the subtraction terms $\lambda_l{}^{I}(s)$. The value of $a_1{}^1$ was calculated from the Gribov-Froissart representation:

$$a_1{}^1 = \frac{4}{3\pi} \int_4^{47} \frac{dx}{x^2} \left[\frac{\operatorname{Im} f_0{}^0(x)}{3} + \frac{3}{2}\left(\frac{x+4}{x-4}\right) \operatorname{Im} f_1{}^1(x) - \frac{5}{6} \operatorname{Im} f_0{}^2(x) \right]$$

$$+ (1.31 \pm 0.16) \cdot 10^{-1}. \tag{13}$$

Substituting the experimental values of $\operatorname{Im} f_l{}^{I}(x)$ we obtained $a_1{}^1 = (0.034 \pm 0.003) \mu^{-3}$. Using $a_1{}^1$, it is possible to calculate $(2a_0{}^0 - 5a_0{}^2)$. To this end, we used the transformed Wanders representation

$$(2a_0{}^0 - 5a_0{}^2) = 18a_1{}^1 + \int_4^{47} \left[2 \operatorname{Im} f_0{}^0(x) - 5 \operatorname{Im} f_0{}^2(x) \right.$$

$$\left. - \frac{9(3x-4)}{x-4} \operatorname{Im} f_1{}^1(x) \right] \frac{dx}{x^2(x-4)} - (8.6 \pm 4.3) \cdot 10^{-3}. \tag{14}$$

The values of $a_0{}^0$ were fixed in the interval $-0.05 \leq a_0{}^0 \leq 0.6 \mu^{-1}$ and the $\operatorname{Re} f_l{}^{I}(s)$ were calculated. A comparison of the solutions with the experimental points was carried out in accord with the χ^2 criterion.

Since the P_1 wave is not very sensitive to changes of $a_0{}^0$, while the values of $\delta_0{}^2$ have not been sufficiently well defined near the threshold, χ^2 was determined from the S_0 wave. We obtained $a_0{}^0 = (0.24 \pm 0.03) \mu^{-1}$. Adding the unitarity requirement (the Roy equations correspond only to analyticity and crossing symmetry), we are left with the region $0.22 \leq a_0{}^0 \leq 0.27 \mu^{-1}$. Figure 8 shows the experimental and calculated values of $\operatorname{Re} f_l{}^{I}(s)$ for $a_0{}^0 = 0.24 \mu^{-1}$. It is seen that the description of all the portional amplitudes is quite good. The behavior of $\operatorname{Re} f_l{}^{I}(s)$ in the unphysical region $-4 < s < 4$ is shown. It is seen that the S-wave amplitudes have subthreshold zeros quite close to the physical region at $s_0 = -0.2$ and $s_2 = 2.4$.
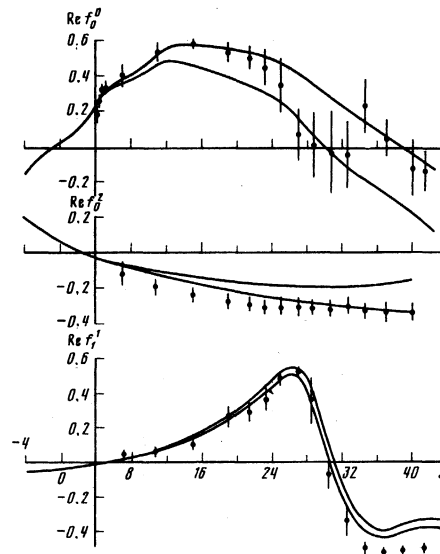

FIG. 8. Comparison of the obtained solutions of the Roy equations at $a_0^0 = 0.24\ \mu^{-1}$ (region between the solid lines) with the experimental real parts of the S- and P-wave amplitudes $\operatorname{Re} f_l^I(s)$.

6. ANALYSIS OF EXPERIMENTAL RESULTS

6.1. Scattering lengths

The S-wave length a_0^0 was determined in a large number of studies, but the results differ greatly. Let us discuss this discrepancy with account taken of our data.

In the present study, a_0^0 was obtained by three independent methods.

1. By applying the effective-radius formulas to the phase shifts δ_0^0 in the near-threshold region $280 \leqslant m_{\pi\pi} \leqslant 320$ MeV: $a_0^0 = (0.24 \pm 0.07)\mu^{-1}$.

2. By using the Serebryakov formulas, which takes into account the existence of a subthreshold zero, for the values of δ_0^0 in the region $280 \leqslant m_{\pi\pi} \leqslant 700$ MeV: $a_0^0 = (0.25 \pm 0.05)\mu^{-1}$.

3. By the method of the Roy equations for the experimental phase shifts δ_0^0, δ_0^2, and δ_1^1 in the region from the threshold to 960 MeV: $0.22 \leqslant a_0^0 \leqslant 0.27\mu^{-1}$. It is seen that the results are in good agreement with one another and the most probable is the value $a_0^0 = (0.24 \pm 0.03)\mu^{-1}$.

If the existence of a subthreshold zero in the S_0 wave close to the physical region, and hence the inapplicability of the effective-radius method to the experimental phase shift at $m_{\pi\pi} \geqslant 400$ MeV, is regarded as proved, then the greater part of the remaining papers yield values of a_0^0 that agree with ours. Thus, in the latest paper on K_{e4} decay[27] the value obtained is $a_0^0 = (0.26 \pm 0.05)\mu^{-1}$; the application of the dispersion relations to $\pi N \to \pi N$ (Ref. 28) yielded $a_0^0 = (0.26 \pm 0.09)\mu^{-1}$; the results of a joint description of the data of the K_{e4} decay and of $\pi^- p \to \pi^- \pi^+ n$ by an equation that takes into account the subthreshold zero yielded $a_0^0 = (0.23 \pm 0.05)\mu^{-1}$ (Ref. 29). It is difficult to explain the large S-wave amplitude obtained at threshold in a number of studies of $\pi^- \pi^+ \to \pi^0 \pi^0$ scattering, and consequently the large $a_0^0 \sim (0.5 - 0.8)\mu^{-1}$ (Refs. 30 and 31). This is possibly due to some systematic error resulting from the complexity of the corresponding experiments. We note that in not all the $\pi^0 \pi^0 n$ studies were large a_0^0 obtained—in Ref. (32) the value is $a_0^0 = (0.15 \pm 0.08)\mu^{-1}$.

The S-wave lengths are strongly correlated with one another. This was first pointed out by Morgan and Shaw,[33] who noted that the S-wave values corresponding to possible solutions in the dispersion-relation approach are located in a narrow region on the (a_0^0, a_0^2) plane. This region is called "universal curve." Figure 9 shows calculations of the universal curve from a number of papers, as well as our experimental region obtained by averaging the results in the method of the Roy equations $(a_0^2 = (-0.02 \pm 0.02)\mu^{-1})$ and from Serebryakov's formula $(a_0^2 = (-0.07 \pm 0.03)\mu^{-1})$. It is seen that the region fits the universal curve well.

The P_1-wave scattering length a_1^1 obtained in the present paper lies in the usual region $a_1^1 = (0.034 \pm 0.003)\mu^{-3}$. Practically all the papers yield close values of a_1^1. An exception is the paper by Manner[34] in which $a_1^1 \sim 0.1\mu^{-3}$. It seems to us that since the absolute value
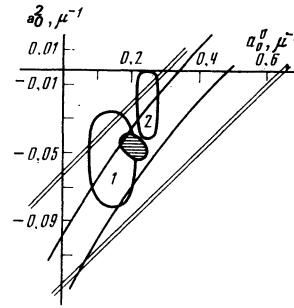

FIG. 9. "Universal curve" on the (a_0^0, a_0^2) plane. The double lines limit the region of possible values from Ref. 25, the region between the solid lines contains the corresponding data from Ref. 45. Shaded region—predictions of the Weinberg "soft-pion" model, region 1—experimental results of Ref. 26. Region 2—result of present paper.

of δ_1^1 is very small, it is difficult to determine it at the required accuracy $\sim 0.1°$, and calculations of the type by the Roy method seem more reliable. It appears that the most promising in the future are the studies of $e^+ e^- \to \pi^+ \pi^-$ at energies close to threshold.

Wavelengths with error $l \geqslant 2$ are small, and there are few exact data for them. Until recently, even the sign of a_2^2 was not established. The review by Nagels et al.[35] cites the value $a_2^2 = (1.3 \pm 3.0) \cdot 10^{-4}\mu^{-5}$. Our data favor a positive sign $a_2^2 = (3.8 \pm 1.4) \cdot 10^{-4}\mu^{-5}$. To conclude the section, we present the obtained scattering lengths:

$$a_0^0 = (0.24 \pm 0.03)\mu^{-1}, \quad a_0^2 = (-0.04 \pm 0.04)\mu^{-1}, \quad a_1^1 = (0.034 \pm 0.003)\mu^{-3},$$
$$a_2^0 = (7.8 \pm 6.0) \cdot 10^{-4}\mu^{-5}, \quad a_2^2 = (3.8 \pm 1.4) \cdot 10^{-4}\mu^{-5}. \tag{15}$$

6.2. The $\pi\pi$-scattering phase shift in the elastic region

We regard one of the most interesting results of the present paper to be the continuity of the phase shift δ_0^0 from the threshold to $m_{\pi\pi} = 960$ MeV. The values of δ_0^0 near threshold were previously obtained by a different procedure and the question whether the data at the threshold can be continued to match the results at large $m_{\pi\pi}$ remained open. Figure 10 shows the values of the δ_0^0 phase shift obtained from one reaction $\pi^- p \to \pi^- \pi^+ n$
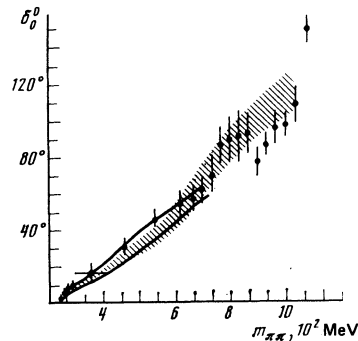

FIG. 10. Values of phase shift δ_0^0 from the reaction $\pi^- p \to \pi^- \pi^+ n$ in the region $280 \leqslant m_{\pi\pi} \leqslant 980$ MeV. Shaded region—calculation by the Roy-equations methods for $a_0^0 = 0.24 \, \mu^{-1}$, region between solid lines—predictions of the model with broken chiral symmetry.[36]

by a unified calculation procedure. It is seen that the δ_0^0 phase shift has a smooth behavior, and that the phase shifts near threshold obtained from emulsion data agree well with the values at $320 \leq m_{\pi\pi} \leq 960$ MeV obtained at $p_\pi = 4.5$ GeV/c with a bubble chamber. The figure shows also the plotted theoretical calculations. The shaded region is the result of calculation by the method of the Roy equations for $a_0^0 = 0.25\ \mu^{-1}$, the region between the solid lines shows the calculation of the behavior of δ_0^0 in the theory of broken chiral symmetry.[36] The agreement between the theory and experiment is good, and it appears that the obtained values of δ_0^0 describe $\pi\pi$ scattering quite correctly up to $m_{\pi\pi}$ = 750 MeV. As already mentioned, there are two possibilities, "up" and "down" solutions. The upper "up" solution leaves a possibility for the existence of the $\epsilon(750)$ resonance.

Our energy-independent analysis did not reveal a possibility of choosing between one of the two existing solutions. In the energy-dependent analysis we obtained the lower solution. In the calculation with the Roy equations the lower solution has $\chi^2/n = 1.0$, whereas for the upper solution $\chi^2/n = 3.5$. Of course, this result does not exclude the upper solution, but is an argument favoring the lower. It seems to us that if we analyze the available pertinent data on this problem, the lower solutions seems at present preferable. The main arguments in its favor are the following.

1) The upper solution predicts a drop in the $\pi^0\pi^0$ cross section, something not confirmed by the existing data.[30,37,38]

2) Searches for the $\epsilon(750)$ meson that corresponds to the upper solution were not successful.[39,40]

3) The lower solution explains naturally the anomaly in $\langle Y_1^0 \rangle$ for the $\pi^-\pi^+ \to \pi^-\pi^+$ scattering near the $K\bar{K}$ threshold.[41,42]

4) The energy-dependent and model-dependent analyses led to the lower solution.[1,14,33]

5) It is impossible to describe the upper solution in the Roy-equations approach.[26] The final answer as to
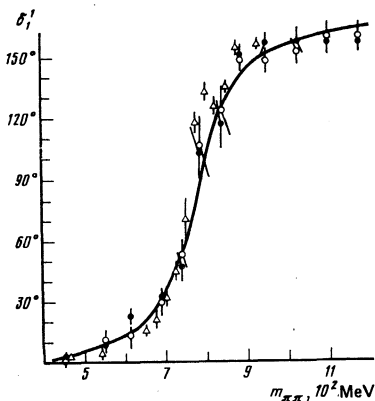

FIG. 12. Values of δ_0^2 from the present paper (points) and from Refs. 3 (■), 46 (□), 47 (△), 48 (○), and 49 (▲). Shaded region—calculation by the Roy-equations method, region between solid lines—result of energy-dependent analysis from the present apper.

which of the solutions is correct can apparently be obtained only from exact data on the $\pi^0\pi^0$ cross section, but at present the lower solution seems desirable.

In the remaining phase shifts there are no such ambiguities in the investigated region. Figure 11 shows the values of the δ_1^1 phase shifts obtained from elastic $\pi^-\pi^+$, $\pi^-\pi^0$, and $\pi^+\pi^0$ scattering. The comforting fact is that the data from different channels are in good agreement with one another. Of course, the δ_1^1 phase shift points to a ρ resonance. Its description by the Breit-Wigner formula

$$\mathrm{tg}\,\delta_1^1 = \frac{m_\rho\Gamma_\rho}{m_\rho^2 - m_{\pi\pi}^2}\left(\frac{q}{q_\rho}\right)^3\left(\frac{1+q_\rho^2 R^2}{1+q_\rho^2 R^2}\right) \qquad (16)$$

yields the parameters $m_\rho = (782.3 \pm 4.4)$ MeV, $\Gamma_\rho = (140.1 \pm 8.6)$ MeV, and $R = (4.1 \pm 1.4)$ GeV^{-1}.

The behavior of the S_2 wave in general outline has been known for a long time, and the phase shift of this wave is negative and small. Figure 12 shows a summary of the values of the phase shift δ_0^2 (the points are the results of the present paper). The shaded region was the result of the phenomenological calculation by the Roy method. At agreement between all the quanti-

FIG. 11. Values of δ_1^1. Points—data of $\pi^-\pi^0 \to \pi^-\pi^0$ scattering, circles—of $\pi^+\pi^0 \to \pi^+\pi^0$ scattering, triangles—of $\pi^-\pi^+ \to \pi^-\pi^+$ scattering. Solid curve—approximation of the phase shift by the relativistic Breit-Wigner formula.
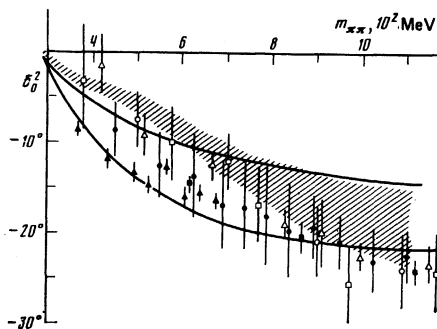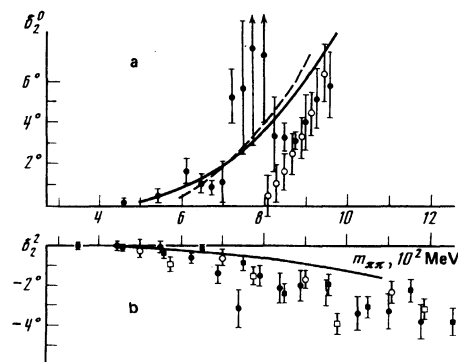

FIG. 13. a) D_0-wave phase shift δ_2^0. Points—from the present paper, circles—from Ref. 43, solid and dashed lines—energy-dependent solutions from Refs. 44 and 1, respectively; b) D_2-wave phase shift δ_2^2. Points—from present paper, ■—from Ref. 3, ○—Ref. 48, □—Ref. 46. Solid line—calculation by the method of the Roy equations from Ref. 25.

ties is satisfactory, although finally, it would be desirable to know δ_0^2 with better accuracy.

Figure 13 shows the D-wave phase shifts δ_2^2 and δ_2^0. The points are the results of the present study. It is seen that δ_2^2 has an easily understood shape, decreasing slowly from $\sim(-0.5)°$ at 600 MeV to $\sim(-4°)$ at 1200 MeV. In our data on the δ_2^0 phase shift there is a certain rise at $m_{\pi\pi} \sim 750$ MeV, which agrees qualitatively with the results of Estabrooks and Martin.[44] At the presently available statistical accuracy, however, we cannot state that the effect is not a result of the method. On the whole, δ_2^0 is positive and increases from 0.5° at 500 MeV to $\sim5°$ at 950 MeV.

[1]B. Hyams, C. Jones, P. Weilhammer, et al., Nucl. Phys. B64, 134 (1973).

[2]P. Estabrooks and A. D. Martin, ibid. B95, 322 (1975).

[3]W. Hoogland, S. Peters, G. Grayer, et al., Nucl. Phys. B157, 250 (1979).

[4]M. J. Corden, J. D. Dovell, J. Garvey, et al., ibid. B157, 250 (1979).

[5]A. A. Kartamyshev, K. N. Mukhin, A. S. Romantseva, et al., Phys. Lett. 44B, 310 (1973).

[6]A. A. Kartamyshev, K. N. Mukhin, O. O. Patarakin, et al., Pis'ma Zh. Eksp. Teor. Fiz. 23, 478 (1976) [JETP Lett. 23, 432 (1976)].

[7]E. A. Alekseeva, A. A. Kartamyshev, V. K. Makar'in, et al., Pis'ma Zh. Eksp. Teor. Fiz. 29, 109 (1979) [JETP Lett. 29, 100 (1979)].

[8]A. A. Bel'kov, S. A. Bunyatov, K. N. Mukhin, et al., Pis'ma Zh. Eksp. Teor. Fiz. 29, 652 (1979) [JETP Lett. 29, 597 (1979)].

[9]E. A. Alekseeva, A. A. Kartamyshev, V. K. Makar'in, et al., Preprint IAE-3241/1, 1980.

[10]A. A. Kartamyshev, K. N. Mukhin, A. S. Romantseva, et al., Preprint IAE-2374, 1974.

[11]Yu. A. Batusov, S. A. Bunyatov, V. S. Kurbatov, et al., Yad. Fiz. 1, 526 (1965) [Sov. J. Nucl. Phys. 1, 374 (1965)].

[12]A. M. Baldin, V. I. Gol'danskiĭ, and I. L. Rozental', Kinematika yadernykh reaktsiĭ (Kinematics of Nuclear Reactions), Atomizdat, 1968.

[13]J. D. Kimel and E. Reya, Nucl. Phys. B58, 513 (1973).

[14]B. Oh, A. Garfinkel, R. Morse, et al., Phys. Rev. D1, 2494 (1970).

[15]L. Van Hove, Nucl. Phys. B9, 331 (1969).

[16]J. E. Richey, V. Hagopian, J. D. Kimel, et al., Phys. Rev. D15, 3155 (1977).

[17]G. Chew and F. Low, Phys. Rev. 113, 1640 (1959).

[18]J. B. Baton, G. Laurens, and J. Reignier, Phys. Lett. 33B, 525 (1970).

[19]V. V. Serebryakov, Hadron Interactions at Low Energies.

[20]Proc. Triangle Meeting, VEDA Publ. House, Bratislava, 1975.

[20]V. V. Serebryakov and D. V. Shirkov, Phys. Lett. 25B, 138 (1967).

[21]V. R. Garsevanishvili and D. V. Shirkov, Shkola molodykh uchenykh po fizike vysokikh énergiĭ (Young Scientists' School of High-Energy Physics), Sukhumi, 1972, p. 268.

[22]J. Franklin, Phys. Rev. D11, 513 (1975).

[23]S. M. Roy, Phys. Lett. 35B, 353 (1971).

[24]J. L. Basdevant, J. C. Le Guillou, and H. Navelet, Nuovo Cimento 7A, 363 (1972).

[25]J. L. Basdevant, C. G. Groggatt, and J. L. Petersen, Nucl. Phys. B72, 413 (1974).

[26]M. R. Pennington and S. D. Protopopescu, Phys. Rev. D7, 1429 (1973).

[27]L. Rosselet, P. Extermann, J. Fischer, et al., Phys. Rev. D15, 574 (1977).

[28]G. E. Hite and R. J. Jacob, Nucl. Phys. B134, 291 (1978).

[29]A. A. Bel'kov and S. A. Bunyatov, Yad. Fiz. 29, 1295 (1979) [Sov. J. Nucl. Phys. 29, 666 (1979)].

[30]M. David, G. Villet, R. Ayed, et al., Phys. Rev. D16, 2027 (1977).

[31]J. F. Grivaz, P. Davis, R. Ayed, et al., Phys. Lett. 61B, 400 (1976).

[32]K. J. Braun and D. B. Cline, Phys. Rev. D8, 3794 (1973).

[33]D. Morgan and G. Shaw, Phys. Rev. D2, 520 (1970).

[34]W. Manner, in: AIP Conf. Proc. No. 21, Boston, 1974, p. 22.

[35]M. M. Nagels, J. J. de Swart, et al., Nucl. Phys. B147, 189 (1979).

[36]A. A. Bel'kov, V. N. Pervushin, and S. A. Bunyatov, JINR Preprint R2-12636, 1979.

[37]W. D. Apel, J. S. Ausländer, H. Müller, et al., Phys. Lett. B41, 542 (1973); B57, 398 (1973).

[38]D. M. Binnie, Phys. Rev. D8, 2789 (1973).

[39]J. Carroll, J. Matthews, W. D. Walker, et al., Phys. Rev. D10, 1430 (1974).

[40]J. Banaigs, J. Berger, et al., Nucl. Phys. B105, 52 (1976).

[41]S. Flatte, M. Alston-Garnjost, et al., Phys. Lett. B36, 152 (1971); B38, 232 (1972).

[42]D. M. Binnie, Phys. Rev. Lett. 31, 1534 (1973).

[43]S. Protopopescu, M. Alston-Garnjost, and A. Barbaro-Galtieri, Phys. Rev. D7, 1979 (1973).

[44]P. Estabrooks and A. D. Martin, Nucl. Phys. B79, 301 (1974).

[45]D. Trelani and C. Verzegnassi, Lett. Nuovo Cimento 19, 117 (1977).

[46]D. Cohen, T. Ferbel, P. Slattery, et al., Phys. Rev. D7, 662 (1973).

[47]G. V. Beketov, S. M. Zambkovskiĭ, A. B. Kaĭdalov, et al., Yad. Fiz. 19, 1032 (1974) [Sov. J. Nucl. Phys. 19, 528 (1974)].

[48]N. B. Durysoy, M. Baubillier, et al., Phys. Lett. 45B, 517 (1973).

[49]J. P. Prukop, O. R. Sander, J. A. Poitier, et al., Phys. Rev. D10, 2055 (1974).

Translated by J. G. Adashko

600   Sov. Phys. JETP 55(4), April 1982

Alekseeva et al.   600